

# A New Vehicle Detection Approach in Traffic Jam Conditions

Bing-Fei Wu, Jhy-Hong Juang, Ping-Tsung Tsai, Ming-Wei Chang, Chung-Jui Fan, Shin-Ping Lin, Jennifer Yuh-Jen Wu and Hsia Lee

Department of Electrical and Control Engineering, National Chiao Tung University,  
1001 Ta-Hsueh Road, Hsinchu 30050, Taiwan  
Email: bwu@cc.nctu.edu.tw

**Abstract** –The well-known vehicle detectors utilize the background extraction methods to segment the moving objects. The background updating concept is applied to overcome the luminance variation which results in the error detection. These systems will meet a challenge when detecting the vehicles in the traffic jam conditions at sunset. The vehicles will cover the road surface so that the background information cannot be smoothly updated. Once the traffic is released, the existing background is not suitable for the moving segmentation. The main contribution of this paper is that an efficient vehicle detection approach is proposed to improve the detection accuracy in traffic jam conditions. The land mask decision gives the land information and the merged boundary box rule is presented to realize vehicle detection. The signed square normalized correlation coefficient calculation is addressed, and it is applied to vehicle tracking. The experimental results show that this approach works well in highway and urban area with high accuracy.

**Keywords** – Vehicle Detection, traffic jam, tracking.

## I. INTRODUCTION

Traffic information provides the drivers with useful messages for their traveling. For this idea, the vehicle detector is developed to collect the traffic information automatically. There are many sensing technologies applied in vehicle detectors, such as the loop ones, the microwave ones, the infrared one, and the image based ones, etc. In these detectors, the real-time image processing with CCD cameras is applicable and with a low cost for the installation and maintain.

In the recent vision-based vehicle detection processing, virtual slit [1] and virtual loop [2] exploit the concept of inductive loop [3] to detect vehicle passing by monitoring illumination change in pre-specified regions in the frame. Since this kind of processing only checks the pre-specified regions, it gains a faster frame rate. However, it is hard to setup, expensive, and with limited functions. Another type of processing uses double-difference operator [4] with gradient

magnitude to detect vehicles. Although this method consumes more computing time than the one in the previous work, it can gather more vehicle information. However, it has poor performance for adapting the luminance changes caused by lighting condition, or automatic electric shutter (AES). Consequently, optical flow based techniques which estimate the intensity motion between two subsequent frames is used to overcome the change of luminance [5]. However, it requires much more computing time to find out an optimal solution. Hence, Smith *et al.* [7], Brandt *et al.* [8] and Papanikolopoulos *et al.* [9] presented the dynamic update for the background to detect the moving objects. It can adapt the luminance changes in real-time. All of these investigates need the pure initial background image without vehicles inside for the follow-up processing.

In [11,12], the multiple-vehicle detection and tracking (MVDT) system which utilizes a color background to segment moving objects and exploits the relations among the moving objects and existed trajectories for vehicle tracking is proposed. The background information is extracted by the appearance probability of each pixel's color information. And then, it is regularly updated to guarantee the robust segmentation in luminance-change circumstance. MVDT system consists of the dynamic segmentation and the rule-based tracking algorithm shown in Fig.1.

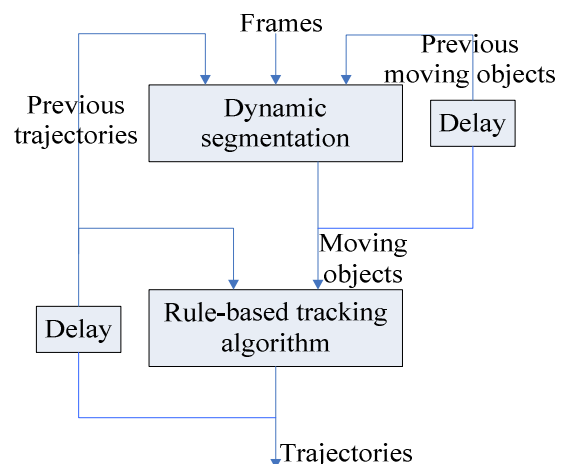


Fig.1. The block diagram of MVDT system [11, 12]

However, the vehicles will cover the road surface or move slowly in traffic jam so that the background is hard to be updated. Once the traffic is released, the existed background is totally not suitable for the follow-up moving object segmentation. To solve this problem, an efficient vehicle detection approach is proposed to improve the detection accuracy in traffic jam conditions in this paper. The lane mask decision gives the lane information and the merged boundary box rule is presented to realize vehicle detection. The signed square normalized correlation coefficient calculation is addressed, and it is applied for vehicle tracking. The experimental results show that this approach works well in highway and urban area with high accuracy.

This paper is organized as follow : Section II addresses the flowchart of the vehicle detection in traffic jam condition. Section III is the lane detection for trajectory direction. The merging processing for vehicle detection is given in Section IV. The vehicle tracking algorithm by Signed Square Normalized Correlation Coefficient calculation is presented in Section V. Finally, the experimental results are given in Section VI and the conclusion is stated in Section VII.

## II. VEHICLE DETECTION IN TRAFFIC JAM CONDITIONS ALGORITHM

Figure 2 is the flowchart of the proposed vehicle detection approach in traffic jam conditions (VDTJ), which is only processed in the trapezoid detection zone (DZ) in Fig.3. The upper bound of this region is arranged in the middle of the scene. In this DZ, lane information is observed since the CCD camera is equipped for forward-looking scenes. The DZ is separated automatically by lane detection to give the trajectory for vehicle detection. VDTJ aims at the moving outline (MO) information to extract the automobiles directly instead of using the processes between the background and current images. The MO is yielded from the difference between two successive images on moving objects. The merged boundary box rule (MBBR) is utilized to recognize these MOs for clustering the vehicles lane by lane. The autos in jam conditions on the roadway move slowly so that the correlation coefficient calculation is brought to track the vehicles, since the vehicles own the similar size and the same contour in the near continuous images.

## III. LANE MARK DETECTION

The pixel on the grabbed image  $P(x, y)$  is a vector with three RGB color components  $[P_R(x, y) P_G(x, y) P_B(x, y)]^T$ . The lane mask  $LMC(x, y)$  is derived from the color information of  $P(x, y)$  either white or yellow lane markings. The lane marking conditions in DZ are obtained using

$$LMC(x, y) = \begin{cases} 1 & P_R(x, y) > THW \text{ and} \\ & P_G(x, y) > THW \text{ and} \\ & (P_B(x, y) > THW \text{ or } P_B(x, y) < THY), \\ 0 & \text{otherwise.} \end{cases}$$

where  $THW$  is a threshold used to check whether the three color components of a background pixel are sufficiently large, and  $THY$  is another threshold applied to check whether the blue component (the complement of yellow) sufficiently small.

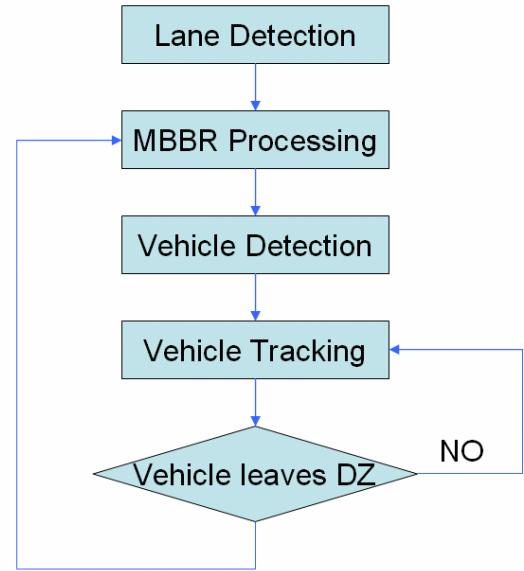


Fig.2. Flowchart of VDTJ

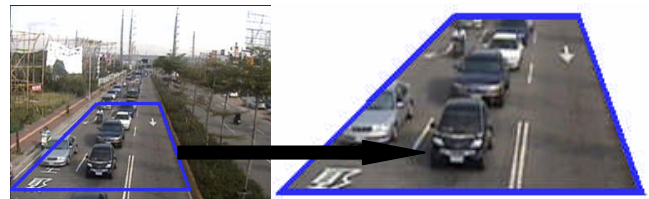


Fig.3. (a) The original image ; (b)The trapezoid DZ

Next, each pixel in  $LMC(x, y)$  is scanned from left to right, bottom to top, to yield the bottom-left coordinate,  $LSS(s)$ :  $(LSS_x(s), LSS_y(s))$ , and the top-left coordinate,  $LSE(s)$ :  $(LSE_x(s), LSE_y(s))$ , of the  $s^{th}$  straight line segment.  $LSS(s)$  must be a coordinate of a start point, specified by the first “1” found at the beginning of a horizontal scan or the “1” following the end of a sequence of “0”s’ in the middle of the scanning. If the number of the sequence of “1”s’ after  $LSS(s)$  (including  $LSS(s)$  itself) is less than a threshold  $TH3$ , the sequence of “1”s’ will be removed. Otherwise, the coordinates will be assigned to  $LSS(s)$ . Thereafter, three types

of vertical connection, displayed in Fig.4, must be considered to determine  $LSE(s)$ , as follows.

1. Assign  $LSE(s)$  as  $LSS(s)$ .
2. Check whether one of the coordinates:  $(LSE_x(s) - 1, LSE_y(s) - 1)$ ,  $(LSE_x(s), LSE_y(s) - 1)$ , or  $(LSE_x(s) + 1, LSE_y(s) - 1)$  owns a start point or not.
3. If step 2 is yes, assign  $LSE(s)$  to the coordinate of the start point and back to step 2.
4. Otherwise, set  $s$  to  $s + 1$ .

During the scanning, each scanned pixel is given a processed flag so that it will not be re-processed in the follow-up processes.

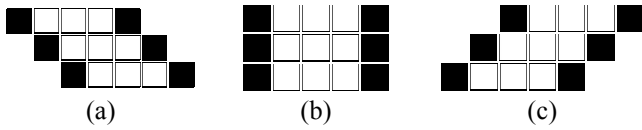


Fig. 4. Vertical connection types; (a) left-hand; (b) front; (c) right-hand

Then, a line segment merging procedure will be adopted to group line segments into separators. As shown in Fig.5, the line segments are imaged as the lane markings and the separators are as the lane boundaries.

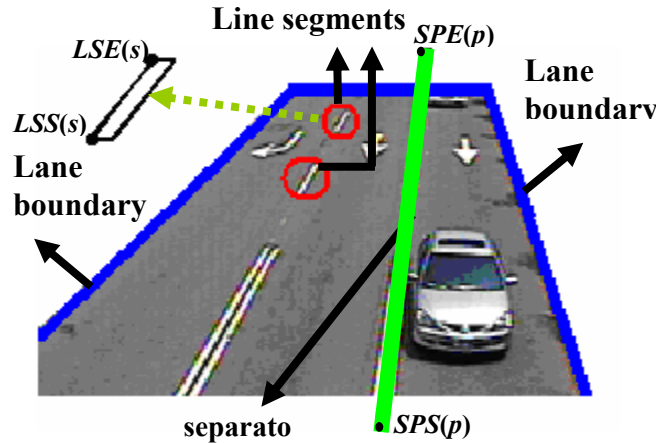


Fig.5. Illustrations of line segments, lane boundaries and separators

Assume the start and end coordinates of the  $p^{\text{th}}$  separator shown in vector form are  $SPS(p) = [SPS_x(p), SPS_y(p)]^T$  and  $SPE(p) = [SPE_x(p), SPE_y(p)]^T$ , respectively. Given a threshold  $TH4$ , the slope of the  $s^{\text{th}}$  line segment is  $LSD(s) = LSE(s) - LSS(s)$  and the slope of the  $p^{\text{th}}$  separator is  $SPD(p) = SPE(p) - SPS(p)$ . The difference between the slopes of the detected  $LSS(s)$  and the existing  $SPE(p)$  is denoted as  $SLD(s, p) = SPE(s) - LSS(p)$ . Once  $|SLD(s, i) - SPD(i)| \leq TH4$ , where  $i = [0, p]$ ,  $SPE(i)$  will be updated to  $SPE(i) = LSE(s)$ . A new

separator is created when  $|SPD(i) - LSD(i)| \geq TH4$  or  $|SLD(i) - LSD(i)| \geq TH4$ , where  $i = [0, p]$ .

Figure 6 shows the lane mask created for the following detections where two boundaries and two separators are involved. The three blocks, Lane 1, Lane2 and Lane3 were addressed as the three lane region for the vehicle detection and illustrated with different gray level values.

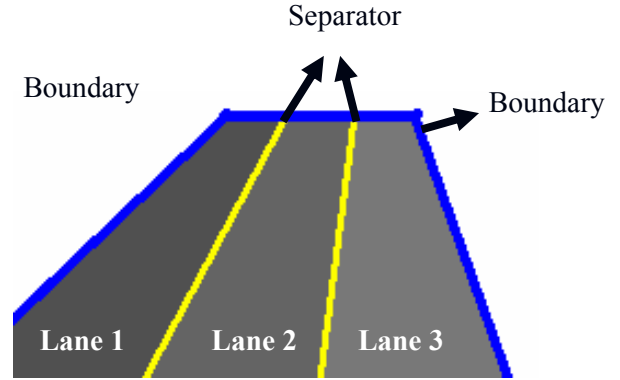


Fig.6. The detected lane mask

#### IV. MBBR PROCESSING AND VEHICLE DETECTION

A color image can be transferred to a gray level one by the model,  $Y = 0.299R + 0.587G + 0.144B$ . It is observed that the green component (G) of the RGB model contributes around 60% to Y in this transformation. Therefore, we only adopt the G plane of the image as the processing target to save the transformation burden. Figure 7 shows two continues images and the MO is obtained in DZ by the difference between the G plane information of these two images, as shown in Fig. 8.



(a) The previous frame (b) The current frame  
Fig.7. Two continuous images

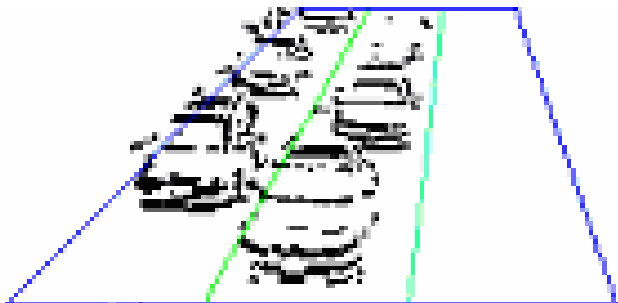


Fig.8. Moving outline in the DZ obtained by the difference between the two frames in Fig.7

The MO will be classified to many small rectangle boundary boxes (RBB) in this procedure. MBBR is presented to merge the overlapped RBB into a large one. Every RBB owns its bottom-left and top-right points and those are denoted as  $(x_{LB1}, y_{LB1})$  and  $(x_{RT1}, y_{RT1})$ , respectively. If two RBBs overlapped, a new RBB is formed to combine and replace the two ones. In Fig. 9, RBB1 and RBB2 overlapped and the new one, RBB4 is made. In the same way, RBB5 is allocated from the merging of RBB3 and RBB4.

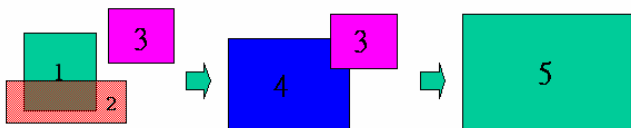


Fig.9. The example for RBB merging processing

Figure 10 is the flowchart of MBBR process and Fig.11 is an example for this process. First, a square box with  $L$  width is set as the initial RBB. This RBB scans in its surroundings with a distance of  $(L/2) + 1$  pixels to complete the merging processing. Once the merging process stops, this RBB size is checked with a  $TH$  set in (1) to determine whether the RBB is a vehicle or not. The decision rules are shown in (2).

$$TH = \{TH_{RH}, TH_{RL}, TH_{AH}, TH_{AL}, TH_D\} \quad (1)$$

$$\begin{aligned} TH_{RH} &> \text{Height} / \text{Width} > TH_{RL} \\ TH_{AH} &> \text{Area} > TH_{AL} \\ MO \text{ Density} &> TH_D \end{aligned} \quad (2)$$

Table I

The definition of the parameters in (1) and (2)

$TH_{RH}$	The upper bound of the height/width ratio
$TH_{RL}$	The lower bound of the height/width ratio
$TH_{AH}$	The upper bound of the RBB area
$TH_{AL}$	The lower bound of the RBB area
$TH_D$	The density of the MO in the RBB

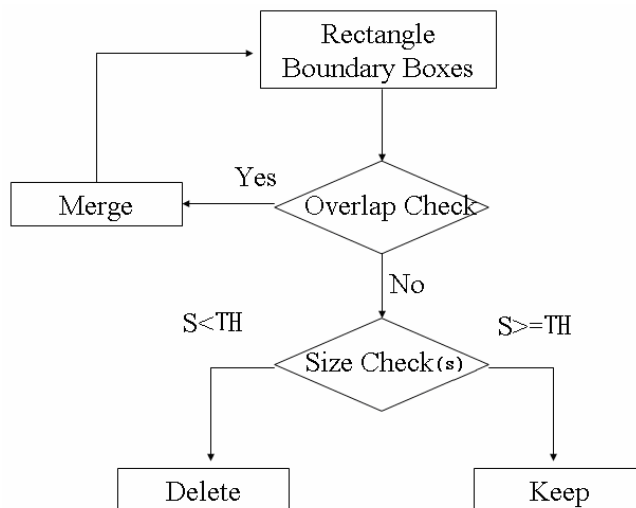


Fig.10. The basic flow for vehicle detection with MBBR

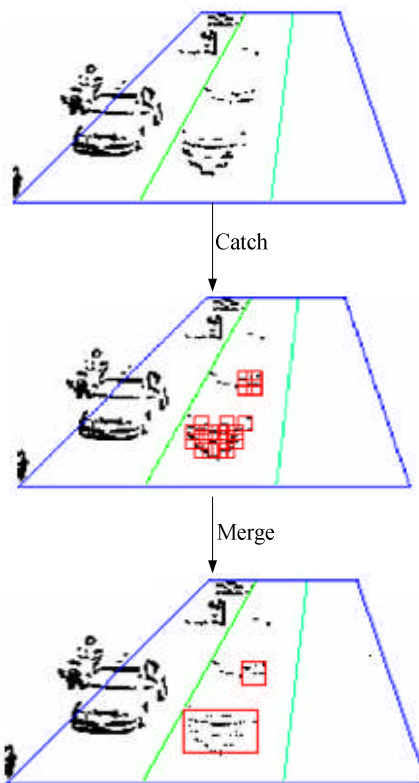


Fig.11. An example for merge rectangles with MBBR



## V. VEHICLSE TRACKING PROCESSING

The vehicle has been extracted after MBBR processing and decision. For the following images, a tracking procedure within the lane is proposed to speed-up the task. The Normalized Correlation Coefficient (NCC) in (3) is used to figure out the similarity.

$$NCC(u_m, v_m, u_s, v_s) = \frac{\sum_{i=-M}^M \sum_{j=-N}^N [m(u_m+i, v_m+j) - \bar{m}] [s(u_s+i, v_s+j) - \bar{s}]}{\sqrt{\sum_{i=-M}^M \sum_{j=-N}^N [m(u_m+i, v_m+j) - \bar{m}]^2 \cdot \sum_{i=-M}^M \sum_{j=-N}^N [s(u_s+i, v_s+j) - \bar{s}]^2}} \quad (3)$$

Table II  
Parameters in Eq. (3)

$m(i, j)$	The pixel (i, j) in previous frame
$s(i, j)$	The pixel (i, j) in current frame
$\bar{m}$	Mean of all pixels for m
$\bar{s}$	Mean of all pixels for s
$u_m, v_m$	The coordinate of the pixel in the frame
$u_s, v_s$	Original position of next frame in ROI
$i, j$	Moving index in ROI for x-axis and y-axis where $-M < i < M$ $-N < j < N$

$$\begin{aligned} & \sum_{i=-M}^M \sum_{j=-N}^N (m_{ij} - \bar{m})(s_{ij} - \bar{s}) \\ &= \sum_{i=-M}^M \sum_{j=-N}^N m_{ij} s_{ij} - \bar{s} \cdot \sum_{i=-M}^M \sum_{j=-N}^N m_{ij} - \bar{m} \cdot \sum_{i=-M}^M \sum_{j=-N}^N s_{ij} + \sum_{i=-M}^M \sum_{j=-N}^N \bar{m} \cdot \bar{s} \\ &= \sum_{i=-M}^M \sum_{j=-N}^N m_{ij} s_{ij} - (2M+1)(2N+1) \cdot \bar{m} \cdot \bar{s} - (2M+1)(2N+1) \cdot \bar{m} \cdot \bar{s} + (2M+1)(2N+1) \cdot \bar{m} \cdot \bar{s} \\ &= \sum_{i=-M}^M \sum_{j=-N}^N m_{ij} s_{ij} - (2M+1)(2N+1) \cdot \bar{m} \cdot \bar{s} \end{aligned} \quad (4)$$

$$\begin{aligned} & \sum_{i=-M}^M \sum_{j=-N}^N (m_{ij} - \bar{m})^2 \\ &= \sum_{i=-M}^M \sum_{j=-N}^N m_{ij}^2 - 2 \sum_{i=-M}^M \sum_{j=-N}^N m_{ij} \bar{m} + \sum_{i=-M}^M \sum_{j=-N}^N \bar{m}^2 \\ &= \sum_{i=-M}^M \sum_{j=-N}^N m_{ij}^2 - 2(2M+1)(2N+1) \bar{m}^2 + (2M+1)(2N+1) \bar{m}^2 \\ &= \sum_{i=-M}^M \sum_{j=-N}^N m_{ij}^2 - (2M+1)(2N+1) \bar{m}^2 \end{aligned} \quad (5)$$

In our procedure, a signed square normalized correlation coefficient (SSNCC) is considered to reduce the computing burden. In (3),  $\sum_{i=-M}^M \sum_{j=-N}^N (m_{ij} - \bar{m})(s_{ij} - \bar{s})$  and  $\sum_{i=-M}^M \sum_{j=-N}^N (m_{ij} - \bar{m})^2$  are represented as (4) and (5) to yield (6).

$$NCC(u_m, v_m, u_s, v_s) = \frac{\sum_{i=-M}^M \sum_{j=-N}^N m_{ij} s_{ij} - (2M+1)(2N+1) \cdot \bar{m} \cdot \bar{s}}{\sqrt{\sum_{i=-M}^M \sum_{j=-N}^N m_{ij}^2 - (2M+1)(2N+1) \bar{m}^2} \sqrt{\sum_{i=-M}^M \sum_{j=-N}^N s_{ij}^2 - (2M+1)(2N+1) \bar{s}^2}} \quad (6)$$

To consider the signed effect, (7) follows (6) and is named Signed Square Normalized Correlation Coefficient (SSNCC) in (7). The closer to 1 the SSNCC is, the more similar the two rectangle objects are.

$$SSNCC(u_m, v_m, u_s, v_s) = \frac{\text{sign} \left( \sum_{i=-M}^M \sum_{j=-N}^N m_{ij} s_{ij} - (2M+1)(2N+1) \cdot \bar{m} \cdot \bar{s} \right) \cdot \left( \sum_{i=-M}^M \sum_{j=-N}^N m_{ij} s_{ij} - (2M+1)(2N+1) \cdot \bar{m} \cdot \bar{s} \right)^2}{\left( \sum_{i=-M}^M \sum_{j=-N}^N m_{ij}^2 - (2M+1)(2N+1) \bar{m}^2 \right) \left( \sum_{i=-M}^M \sum_{j=-N}^N s_{ij}^2 - (2M+1)(2N+1) \bar{s}^2 \right)} \quad (7)$$

The center point of the extracted vehicle,  $V_c(x, y)$ , is assigned as the tracking node of this vehicle. For the next image, the SSNCC of the RBB is calculated in the centralized region  $M$  by  $N$ , where  $M$  and  $N$  are the half of the width and height of the RBB.  $V_c$  will move in the square region  $[x \pm i, y \pm j]$ , where  $i=[0,5]$  in pixel.

## VI. EXPERIMENTAL RESULTS

In these investigations, highway and urban area are the two scenarios for VJTD. The first one is on the National Highway No.1 heading to South at 94 km in Fig. 12. The second one is in the urban area at Hsin-Chu, Taiwan in Fig. 13. The QVGA frame size image sequences are processed in this study.

Table III and Table IV list the detection accuracy rate of these two scenerios. The proposed system is developed on Winows XP platform with a Pentium-4 2.8GHz CPU, 512M RAM. The average accuracy rate is 97.74%. In the highway testing scenerio, the vehicles move slowly, so the traffic is very busy and the distance between vehicles is close. In the urban area, most vehicles stop for waiting the traffic light. It results in the condition that there is almost no distance between the front car and the rear car. Based on the experimental results, we know that VDTJ can detect the vehicles with a good performance in jam conditions.

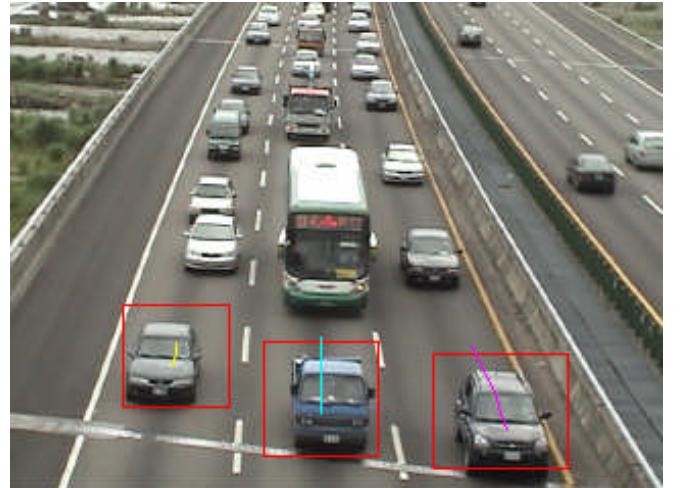


Fig. 12 The highway scenario

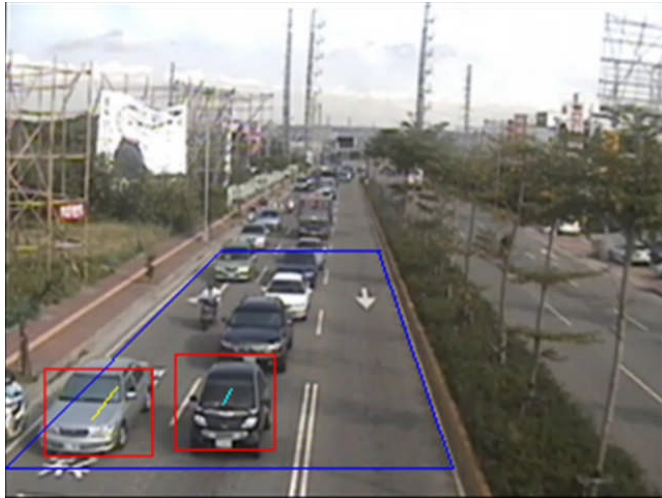


Fig. 13 The urban area scenario

Table III  
Experimental Result for highway

National highway scenario	
Left Lane (Recognized count/ Real Count)	188/194 (96.9%)
Middle Lane (Recognized count/ Real Count)	192/197 (97.46%)
Right Lane (Recognized count/ Real Count)	207/212 (97.64%)
Total (Recognized count/ Real Count)	587/603 (97.35%)
Execution time per frame	23.21msec

Table IV.  
Experimental Result for urban

Urban area scenario	
Left Lane (Recognized count/ Real Count)	24/24 (100%)
Middle Lane (Recognized count/ Real Count)	23/23 (100%)
Right Lane (Recognized count/ Real Count)	14/15 (93.33%)
Total (Recognized count/ Real Count)	61/62 (98.38%)
Execution time per frame	62.88msec

## VII. CONCLUSIONS

In this paper, the vehicle detection system is proposed to solve the vehicle detection in traffic jam conditions. The lane detection is presented to separate the DZ lane by lane for the following processing. This is an automatically processing which can ignore the complex manual setting. The MBBR processing for vehicle detection is a good solution to reconstruct the broken moving outline as a vehicle tracking to enhance the system performance. The VDTJ system will be integrated with the recent background extraction related

investigations to enhance the performance of vehicle detector, especially for the traffic jam conditions.

## ACKNOWLEDGMENT

The work is financially supported by National Science Council under Grant no. NSC 95-2752-E-009 -012 -PAE and Institute of Transportation under Grant no. 951006.

## REFERENCE

- [1] Shunsuke Kamijo, Yasuyuki Matsushita, Katsushi Ikeuchi, Masao Sakauchi, "Traffic monitoring and accident detection at intersections", *IEEE Transactions on Intelligent Transportation Systems*, vol. 1, no. 2, pp. 108-118, Jun. 2000.
- [2] Andrew H. S. Lai and Nelson H. C. Yung, "Vehicle-type identification through automated virtual loop assignment and block-based direction-biased motion estimation", *IEEE Transactions on Intelligent Transportation Systems*, vol. 1, no. 2, pp. 86-97, Jun. 2000.
- [3] Dae-Woon Lim, Sung-Hoon Choi, Joon-Suk Jun, "Automated detection of all kinds of violations at a street intersection using real time individual vehicle tracking", *IEEE International Conference on Image Analysis and Interpretation*, pp. 126-129, Apr. 2002.
- [4] Rita Cucchiara, Massimo Piccardi, and Paola Mello, "Image analysis and rule-based reasoning for a traffic monitoring system", *IEEE Transactions on Intelligent Transportation Systems*, vol. 1, no. 2, pp. 119-130, Jun. 2000.
- [5] Baoxin Li, Rama Chellappa, "A generic approach to simultaneous tracking and verification in video", *IEEE Transactions on Image Processing*, vol. 11, no. 5, pp. 530-544, May 2002.
- [6] Hai Tao, Harpreet S. Sawhney, and Rakesh Kumar, "Object tracking with Bayesian estimation of dynamic layer representations", *IEEE Transactions on Pattern Analysis and Machine Intelligence*, vol. 24, no. 1, pp. 75-89, Jan. 2002.
- [7] Christopher E. Smith, Scott A. Brandt, and Nikolaos P. Papanikolopoulos, "Visual tracking for intelligent vehicle-highway systems", *IEEE Transactions on Vehicular Technology*, vol. 45, no. 4, pp. 744-759, Nov. 1996.
- [8] Surendra Gupte, Osama Masoud, Robert F. K. Martin, and Nikolaos P. Papanikolopoulos, "Detection and classification of vehicles", *IEEE Transactions on Intelligent Transportation Systems*, vol. 3, no. 1, pp. 37-47, Mar. 2002.
- [9] Dieter Koller, Joseph Weber, and Jitendra Malik, "Robust multiple car tracking with occlusion reasoning", *Third European Conference on Computer Vision*, pp. 186-196, Springer-Verlag, 1997.
- [10] Thomas Bücher, Cristobal Curio, Johann Edelbrunner, Christian Igel, David Kastrup, Iris Leefken, Gesa Lorenz, Axel Steinhage, Werner von Seelen, "Image processing and behavior planning for intelligent vehicles", *IEEE Transactions on Industrial Electronics*, vol. 50, no. 1, pp. 62-75, Feb. 2003.
- [11] Chao-Jung Chen, Chung-Cheng Chiu, Bing-Fei Wu, Shin-Ping Lin and Chia-Da Huang, "The Moving Object Segmentation Approach to Vehicle Extraction," in *Proc. IEEE International Conference on Networking, Sensing and Control*, vol. 1, pp. 19-23, Mar. 2004.
- [12] Bing-Fei Wu, Shin-Ping Lin, Yuan-Hsin Chen, "A Real-Time Multiple-Vehicle Detection and Tracking System with Prior Occlusion Detection and Resolution" in *Proc. 5<sup>th</sup> IEEE International Conference on Signal Processing and Information Technology*, Dec. 2005, pp. 311-316.